Regenerative Therapy 30 (2025) 207–216

Contents lists available at ScienceDirect

Regenerative Therapy

journal homepage: http://www.elsevier.com/locate/reth

Original Article

Nanosecond pulsed electric field applications rejuvenate aging endothelial cells by rescuing mitochondrial-to-nuclear retrograde communication

Meifang Yin [a,b,1], Jie Xiao [a,1], Guangtao Huang [a,1], Huanyu Xie [a], Hongwei Liu [c], Jianqiang Yuan [c], Xiaofang Liu [a], Anna Chiarini [b], Ubaldo Armato [b], Ilaria Dal Prà [b], Shumaila Ijaz [a], Naziat Begum [a], Lingyun Wang [c,*], Jun Wu [a,**]

[a] Department of Burn and Plastic Surgery, Medical Innovation Technology Transformation Center, Shenzhen Second People's Hospital, The First Affiliated Hospital of Shenzhen University, Shenzhen 518035, China
[b] Department of Surgery, Dentistry, Pediatrics and Gynecology, University of Verona, 8 Strada Le Grazie, 37134 Verona, Italy
[c] Institute of Fluid Physics, China Academy of Engineering Physics, Mianyang, 621999, China

ARTICLE INFO

Article history:
Received 20 May 2025
Received in revised form
5 June 2025
Accepted 6 June 2025

Keywords:
Nanosecond pulsed electric field
Endothelial aging
Mitochondrial-nuclear communication
Oxidative stress
Vascular regeneration

ABSTRACT

Introduction: Endothelial cell aging is strongly associated with mitochondrial dysfunction, particularly the disruption of mitochondrial-nuclear retrograde communication (MNRC), which is essential for sustaining cellular homeostasis and regulating crucial cellular processes. Nanosecond pulsed electric fields (nsPEF) were shown to exert biological effects by targeting mitochondria. However, the nsPEF regulation of MNRC is still unclear.

Methods: In this study, we set up an *in vitro* model of D-galactose-induced senescence in human umbilical vein endothelial cells (HUVECs) to investigate the effects of nsPEF treatment on oxidative stress, cell proliferation, mitochondrial membrane potential, and markers of MNRC (MNRC), including HIF-1α and SIRT1. Moreover, we conducted *in vivo* animal experiments to evaluate nsPEF treatment's effects on HIF-1α and SIRT1 protein expression in endothelial cells (ECs) of *in vivo* rodents' aging/senescing skin tissue, as well as to examine any later changes in vascular density within the skin.

Results: In vitro results showed that nsPEF treatment suppressed D-galactose-induced senescing effects as they rescued mitochondrial membrane potential, and activated HIF-1α and SIRT1. These effects were confirmed by concurrent reductions in SA-β-Gal activity and in ROS production, and increases in EdU-positive (DNA-synthesizing) cells. Our data showed that nsPEF treatments rescued endothelial cells from D-galactose senescence. Interestingly, nsPEF selectively targeted senescing cells at the tested dose, with no detectable effect on otherwise untreated (normal) HUVECs. In vivo nsPEF treatments upregulated the expression of HIF-1α and SIRT1 in ECs and promoted neoangiogenesis in aged/senescent rodents' skin.

Conclusions: These findings suggest that nsPEF treatments rescue ECs from aging by restoring MNRC, highlighting its potential as a therapeutic strategy for age-related vascular diseases.

Abbreviations: MNRC, mitochondrial-nuclear retrograde communication; nsPEF, nanosecond pulsed electric fields; HUVECs, human umbilical vein endothelial cells; SA-β-Gal, senescence-associated β-galactosidase; ROS, reactive oxygen species; ECs, endothelial cells; VEGF, vascular endothelial growth factor; NO, nitric oxide; ECGS, endothelial cells growth factor; DCFH-DA, diacetyl dichlorofluorescein; SEM, standard error of the mean.

* Corresponding author. China Academy of Engineering Physics, Mianshan Road, No. 64, Mianyang, 621999, China.
** Corresponding author. The First Affiliated Hospital of Shenzhen University, Sungang West Road, No. 3002, Shenzhen 518035, China.
E-mail addresses: 101kpa@sina.com (L. Wang), junwupro@email.szu.edu.cn (J. Wu).
Peer review under responsibility of the Japanese Society for Regenerative Medicine.
[1] These authors contributed equally.

https://doi.org/10.1016/j.reth.2025.06.004

1. Introduction

Endothelial cells (ECs) are particularly susceptible to aging [1], which contributes to vascular dysfunction and plays a critical role in the pathogenesis of various age-related diseases [2], including skin aging [3], delayed wound healing [4], heart failure [5], and neurodegenerative disorders [6]. Cellular aging is defined by a series of hallmarks, including mitochondrial dysfunction, a prominent feature [7]. The latter is a likely key driver of aging phenotypes by operating through various feedback mechanisms, particularly those involving mitochondrial-nuclear retrograde signaling [8]. Several factors, such as reactive ROS, cellular metabolites (e.g., $NADH^{+}$), ATP levels, mitochondrial membrane potential, and Ca^{2+}, primarily modulate this retrograde signaling [9–12]. Mitochondria serve as central signaling hubs that convey information to the nucleus in response to cellular stressors, such as increased ROS production or energy deficits. This communication triggers transcriptional changes that regulate the expression of genes crucial for keeping cellular homeostasis. Disruption of mitochondrial-nuclear signaling impairs fundamental cellular processes such as cell metabolism, proliferation, differentiation, and stress adaptation, all of which contribute to the aging process [8,13].

HIF-1α and SIRT1 are major mediators of MNRC [14]. HIF-1α is a transcription factor that plays a vital role in maintaining cellular homeostasis by regulating genes involved in energy metabolism, angiogenesis, and apoptosis [15,16]. In aging ECs, decreased HIF-1α expression leads to the downregulation of vascular endothelial growth factor (VEGF), impairing vascular repair and angiogenesis [17,18]. Similarly, SIRT1, a NAD^{+}-dependent deacetylase, regulates cellular processes such as mitotic cell cycle, DNA damage response, metabolism, autophagy, and apoptosis [19–21]. Inhibition of SIRT1 in ECs induces an aging-like phenotype and leads to cell cycle arrest [22]. Hence, HIF-1α and SIRT1 play pivotal roles in the pathophysiology of aging ECs [17,23].

In contrast to conventional PEFs, the nsPEF pulse duration is significantly shorter (nanoseconds), falling below the characteristic time needed for cell membrane repolarization. This feature allows nsPEF to penetrate cell membranes and interact with subcellular structures, including the nucleus and mitochondria, thereby inducing various biological effects [24–26]. Yuchen Zhang et al. (2018) proved that nsPEF treatment promotes ECs proliferation in suspension culture, with concurrent changes in intracellular Ca^{2+}, ROS, and nitric oxide (NO) production being linked to the observed effects [27]. These factors are known to activate MNRC, suggesting that nsPEF may play a role in stimulating this pathway.

Therefore, it is reasonable to propose that nsPEF might activate MNRC to mitigate the effects of aging in ECs (Scheme 1). To evaluate this hypothesis, we have used *in vitro* and *in vivo* models of aging ECs and assessed the changes (if any) in critical markers and functions induced by a nsPEF treatment. We intended to gain new insights and highlight novel therapeutic strategies for the management of age-related vascular diseases.

2. Methods

2.1. Experimental animals

The Animal Welfare and Ethics Committee of China Resources Group Co. Ltd. (Shenzhen) approved all animal experiments (Approval No. 202300122). Forty male C57BL/6 mice (6 weeks old) and twenty-four male SD rats (20 months old) were bought from Liaoning Changsheng Biotechnology Co., Ltd. (Experimental Animal Production License: SCXK (Liao) 2020-0001). They were housed in a standard animal care environment at a temperature of 20 ± 2 °C and a relative humidity of 40 %–60 %, with free access to food and water.

2.2. D-galactose-induced aging model and nsPEF treatment in C57 mice

After a typical housing until 2 months of age, the C57BL/6 mice were randomly divided into three groups: (a) the untreated control group, (b) the D-galactose-treated group, and (c) the D-galactose + nsPEF group. Mice in the (b) and (c) groups were injected intraperitoneally with D-galactose (120 mg/kg) every day for 12 weeks. Thereafter, the (c) group mice received daily nsPEF treatment (3 kV/cm) for 14 consecutive days. Each nsPEF treatment lasted for 3 min. While the control group did not undergo any intervention, all mice were anesthetized daily (once a day, for 3 min each time) on the same operation board.

2.3. nsPEF treatment in SD rats

SD rats were randomly assigned to either the untreated control group or the nsPEF treatment group. Rats in the nsPEF treatment group received daily nsPEF treatment (3 kV/cm) for 14 consecutive days, each lasting for 3 min. The control group did not undergo any intervention, but all rats were anesthetized daily (once a day, for 3 min each time) on the same operation board. Fig. 1 shows the electrical models of nsPEF devices for *in vitro* (A) and *in vivo* (B) applications.

2.4. Immunofluorescence staining

Under deep anesthesia, rat skin tissues were collected, fixed with 4 % paraformaldehyde for 24 h, dehydrated, and embedded in paraffin. The skin paraffin blocks were sectioned into 5 μm thick slices. After deparaffinization and antigen retrieval, skin sections were incubated overnight at 4 °C with diluted primary antibodies. After washing three times with PBS (5 min each), sections were incubated with diluted secondary antibodies at room temperature for 60 min. After three more washes, nuclei were stained with DAPI, and the sections were mounted on coverslips using a fluorescence mounting medium (Agilent Technologies, Inc.).

Images were acquired using a Zeiss LSM 800 Confocal Laser Scanning Microscope (Carl Zeiss Microscopy GmbH, Jena, Germany). For each sample, at least three randomly selected non-overlapping fields were imaged per section, and a minimum of three biological replicates were analyzed per group. Fluorescence intensity was quantified using ImageJ software (National Institutes of Health, Bethesda, MD, USA). The fluorescence intensity of each image was recorded individually. All quantitative data were plotted using GraphPad Prism (GraphPad Software, San Diego, CA, USA). Antibody information and dilution concentrations are listed in Table 1.

2.5. Cell culture

HUVECs were bought from FuHeng Biotechnology Co., Ltd. (Shanghai, China). Cells were cultured in ECM complete medium (fortified with 5 % FBS, 1 % ECs growth factor, and 1 % penicillin/streptomycin solution) at 37 °C with 5 % CO_2 in a cell incubator.

2.6. Preparation of aging HUVECs and nsPEF treatment

HUVECs were seeded into 10 cm cell culture dishes (3×10^5 cells per dish) pre-coated with coverslips for 17 h. Then,

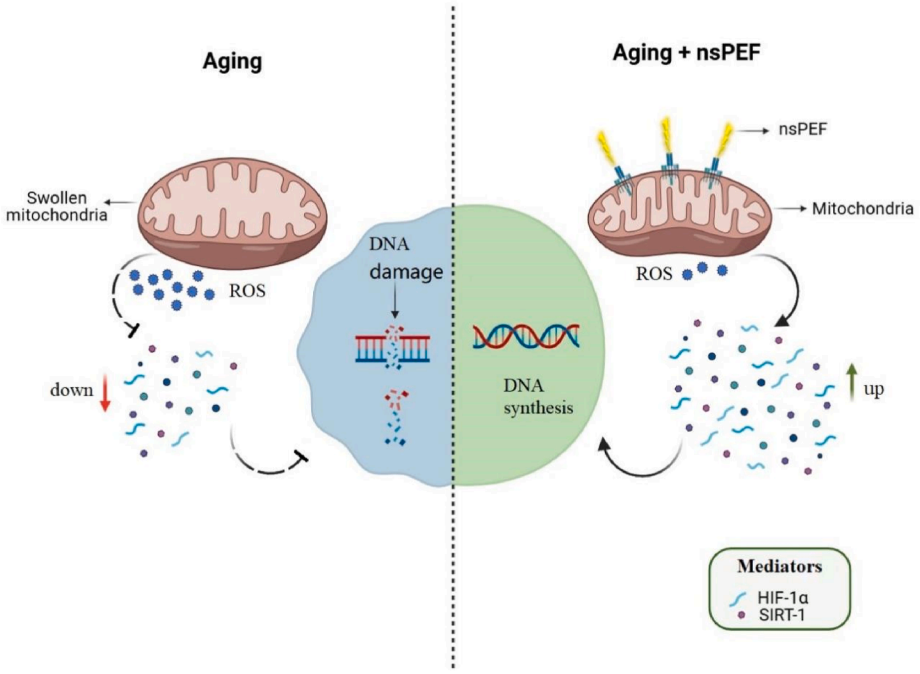

Scheme 1. Illustration of the mechanisms by which nsPEF mitigates the effects of aging in ECs.

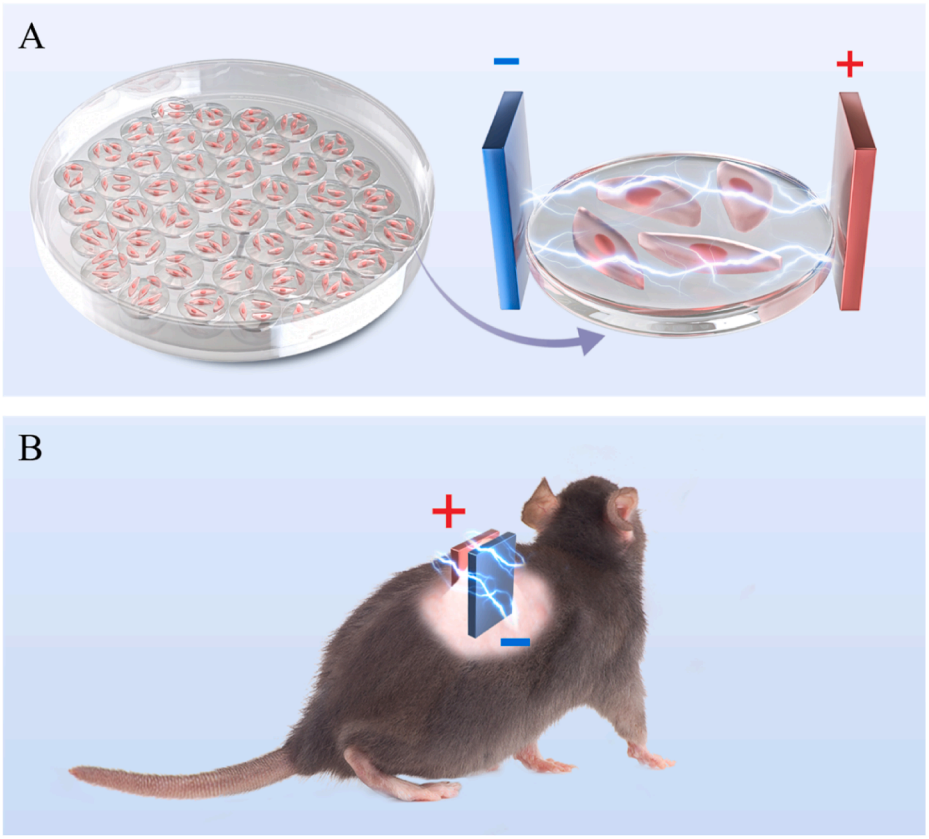

Fig. 1. Electrical models of nsPEF devices used *in vitro* and *in vivo*. (A) Directly applied to *in vitro* cell slides. (B) Directly applied to animal skin for treatment.

cells were incubated with an ECM medium containing 20 g/L D-galactose for 48 h [28], during which the concentration of FBS and ECs growth factor (ECGS) in the ECM medium was halved. Afterward, the coverslips with cells underwent a 3-minnsPEF treatment (3 kV/cm). The electrical models of nsPEF devices for *in vitro* and *in vivo* applications are shown in Fig. 1A.

Table 1
List of antibodies used in this study.

Antibody	Brand	Catalog number	RRID	Concentration	Reactive species
HIF-1α	ABclonal	A22041	AB_3676378	1:200	Human
SIRT1	ABclonal	A0230	AB_2757043	1:200	Human, Mouse, rat
HIF-1α	Absin	abs120168	AB_3676379	1:200	Mouse, rat
CD31	ABclonal	A27114	AB_3676380	1:400	Mouse, rat
α-SMA	Servicebio	GB13044	AB_2942067	1:200	Mouse, rat

2.7. Senescence-associated beta-galactosidase (SA-β-gal) staining

We performed SA -β-Gal staining according to the manufacturer's (Beyotime) instructions to evaluate the effects of nsPEF applications on D-galactose-induced HUVEC aging. The culture medium was removed, and the cells were washed twice with PBS. Cells were fixed at room temperature for 15 min with β-galactosidase fixative solution. After removing the fixative, SA-β-gal staining solution (500 μL per well) was added and incubated at 37 °C without CO_2 for 24 h. Aging HUVECs were stained blue and seen under an inverted microscope (SQS40P, Shenzhen Shengqiang Technology Co., Ltd., China). For each sample, at least three randomly selected non-overlapping fields were imaged per cell culture slide samples. SA-β-gal positive cells were quantified using ImageJ. %SA-β-gal$^+$ cells = number of SA-β-gal positive cells/total number of cells. All quantitative data were plotted using GraphPad Prism.

2.8. Ethynyl-2′-deoxyuridine (EdU) cell proliferation assay [29]

Using the EdU staining kit (Invitrogen) allowed us to assess the ongoing proliferation of HUVECs by labeling their DNA synthesis. After nsPEF stimulation, the cells were cultured in an ECM complete medium for a further 48 h. EdU (final concentration 10 μM) was added (Component A) for 2 h at 37 °C. After 15 min of fixation with 4 % PFA at room temperature, the fixative was discarded. The cells were washed twice with 3 % BSA in PBS and then incubated with 0.5 % Triton X-100 in PBS for 20 min at room temperature. An appropriate amount of Click-iT® reaction cocktail was added according to the instructions, and the cells were incubated at room temperature in the dark for 30 min. Nuclei were stained with DAPI. The cellular specimens were mounted with a fluorescence mounting medium (Agilent Technologies, Inc.), and images were taken under a confocal microscope (ZEISS/LSM800, Germany). For each sample, at least three randomly selected non-overlapping fields were imaged per cell culture slide samples. The percent DNA synthesis fraction rate was calculated as EdU-positive cells/DAPI-positive cells × 100. All quantitative data were plotted using GraphPad Prism.

2.9. Cellular ROS detection

A diacetyl dichlorofluorescein (DCFH-DA) probe was used to detect ROS generation in HUVECs. After nsPEF treatment, cells were cultured for an additional 48 h in an ECM complete medium. The culture medium was removed, and the cells were washed once with PBS. Then, DCFH-DA-containing serum-free ECM medium was added to the samples and incubated at 37 °C for 20 min. After two washes with serum-free DMEM, ROS levels were observed under a confocal microscope (ZEISS/LSM800, Germany). For each sample, at least three randomly selected non-overlapping fields were imaged per cell culture slide samples. ImageJ software served to assess the ROS fluorescence intensity in five randomly selected images. All quantitative data were plotted using GraphPad Prism.

2.10. Mitochondrial membrane potential detection

The JC-1, a cationic carbocyanine dye (green fluorescent) probe, was used to detect changes in mitochondrial membrane potential. A red fluorescence indicates that the mitochondrial membrane potential is high, but when it is low, a green fluorescence is seen. Thus, by observing the color shift of JC-1 fluorescence, any changes in mitochondrial membrane potential can be assessed. After nsPEF treatment, cells were cultured for a further 6 h in an ECM complete medium. After a wash with 1 × PBS, 500 μL of prepared JC-1 staining working solution was added to each well and incubated at 37 °C for 20 min in the dark. After two washes with pre-cooled JC-1 staining buffer at 4 °C, images were taken under a confocal microscope (ZEISS/LSM800, Germany). For each sample, at least three randomly selected non-overlapping fields were imaged per cell culture slide samples. ImageJ software served to assess the fluorescence intensity in five randomly selected images. Calculate the ratio of red fluorescence to green fluorescence. All quantitative data were plotted using GraphPad Prism.

2.11. Immunofluorescence staining of cells on cover slips

For fluorescence staining, cells on coverslips were washed once with 1 × PBS and next fixed in 4 % PFA at room temperature for 15 min. After removing the fixative, the cells were washed three times with pre-cooled 1 × PBS. They were permeabilized with 0.2 % TritonX-100 in PBS at room temperature for 15 min and washed three times with 1 × PBS (3 min each). The cells were then blocked with blocking buffer (10 % goat serum + 1 % BSA) at room temperature for 1 h. Primary antibodies were diluted and incubated at 4 °C overnight. The secondary antibody was diluted 1:1000 in 1 % BSA and incubated at room temperature for 1 h. The cells were washed three times with 1 × PBS (5 min each). DAPI staining was performed for 25 min before mounting the slides. Images were taken under a confocal microscope (ZEISS/LSM800, Germany). For each sample, at least three randomly selected non-overlapping fields were imaged per cell culture slide samples. ImageJ software served to assess the fluorescence intensity in five randomly selected images. All quantitative data were plotted using GraphPad Prism. Table 1 lists the antibody information and dilution concentrations used in the present study.

2.12. Statistical analysis

All data were analyzed using GraphPad Prism software (version 8.0, USA) and expressed as the mean ± standard error of the mean (SEM) from three independent experiments. *T-tests* and one-way ANOVA *post-hoc* Tukey's test served to assess significant differences between groups. P values < 0.05 were considered statistically significant.

3. Results

3.1. Effects of nsPEF on D-galactose-induced aging phenotype features in HUVECs

SA-β-Gal staining was used to verify whether the D-galactose-induced aging model was successfully set up. The results revealed that D-galactose treatment *in vitro* significantly intensified β-galactosidase activity in HUVECs compared to the control group, leading to a 3.05-fold increase ($P < 0.001$) in blue product formation. This showed that D-galactose accelerated the cellular aging process. In contrast, nsPEF treatments effectively suppressed the increase in β-galactosidase activity otherwise brought about by D-galactose, restoring it to normal levels (Fig. 2A).

To further assess the impact of D-galactose on cellular aging, we evaluated key characteristics of metabolic aging, including the decline in cell proliferation and the increase in oxidative stress. The latter were assessed using EdU staining for DNA synthesis and ROS staining for oxidative stress, respectively. Thus, EdU staining analysis showed that the percent fraction of EdU-positive cells decreased from 30.4 % to 21.5 % ($P < 0.001$ *vs*. group Ctrl) in the D-galactose-induced aging HUVECs. However, nsPEF treatments significantly restored the DNA synthetic capacity of aging HUVECs ($P < 0.001$ *vs*. group Gal), with the size of the percent fraction of EdU-positive cells exceeding that of the control ($P < 0.05$ *vs*. group Ctrl) (Fig. 2B). The results of ROS staining showed that D-galactose treatment intensified oxidative stress since fluorescence intensity increased by 1.59 times ($P < 0.001$ *vs*. group Ctrl) in aging HUVECs. Notably, nsPEF treatment effectively alleviated oxidative stress by returning ROS levels of group Gal ($P < 0.001$ *vs*. group Gal) to normal (Fig. 2C). Importantly, nsPEF treatments of the same intensity exerted no effect on ongoing DNA synthesis fraction and oxidative stress levels or β-galactosidase activity in D-galactose-untreated HUVECs (Fig. 1).

3.2. nsPEF treatments restored mitochondrial membrane potential in HUVECs

To assess the effect of nsPEF on mitochondria, we examined mitochondrial membrane potential, a key indicator of mitochondrial health and bioenergetic capacity. After D-galactose induction, HUVECs' mitochondria were dysfunctional, with a decrease in membrane potential revealed by a red-to-green ratio fall of 0.68-fold ($P < 0.001$ *vs*. Ctrl group) due to an increased proportion of green JC-1 monomers. However, nsPEF treatments significantly restored the proportion of red JC-1 aggregates in aging HUVECs, as shown by a marked elevation in mitochondrial membrane potential ($P < 0.05$ *vs*. Gal group), which was restored to normal levels ($P > 0.05$ vs. Ctrl group) (Fig. 3).

3.3. nsPEF treatments reactivated MNRC in HUVECs

To assess whether nsPEF affects the expression of key MNRC proteins, i.e., HIF-1α and SIRT1, in aging HUVECs, we performed

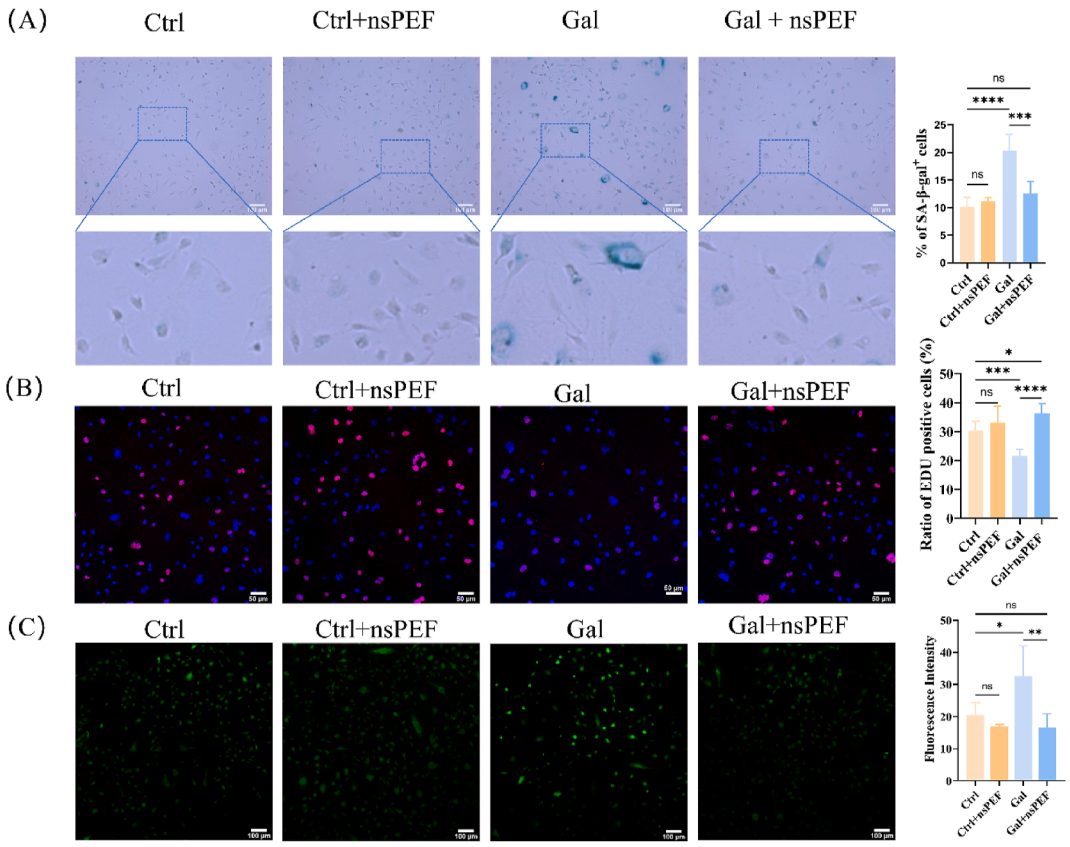

Fig. 2. nsPEF inhibits D-Galactose-induced aging phenotype-related changes but exerts no effects on otherwise untreated (Ctrl) HUVECs. After nsPEF treatments, cells were cultured under normal conditions for 48 h before staining. Ctrl: Normal cultured HUVECs. Ctrl + nsPEF: Normal HUVECs treated with nsPEF, followed by normal culture for 48 h. Gal: Aging HUVECs induced by D-galactose for 48 h, followed by normal culture for 48 h. Gal + nsPEF: Aging HUVECs treated with nsPEF, followed by normal culture for 48 h. (A) SA-β-Gal staining results (scale bar = 200 μm), n = 3 per group. Blue indicates β-galactosidase-positive cells. SA-β-gal positive cells were quantified using ImageJ. %SA-β-gal$^+$ cells = number of SA-β-gal positive cells/total number of cells. (B) EdU staining results (scale bar = 50 μm), n = 3 per group. Red indicates EdU-positive cells. (C) ROS staining results, n = 3 per group. Green indicates ROS-positive cells (scale bar = 100 μm). *$P < 0.05$, **$P < 0.01$, ***$P < 0.001$.

immunofluorescence staining. The fluorescence signal intensity of both proteins was markedly diminished, showing the impairment of MNRC signaling in aging cells. In the D-galactose-induced HUVECs aging phenotype model, nsPEF treatments significantly increased the expression of key MNRC proteins, i.e., HIF-1α (1.45-fold) and SIRT1(3.69-fold) (Fig. 4). Notably, HIF-1α expression went back to normal levels, while SIRT1 expression exceeded that of the normal control.

3.4. nsPEF treatment promotes angiogenesis in aged rodents' skin

As the critical role of angiogenesis in skin aging and regeneration, we thus investigated whether nsPEF could promote angiogenesis in the skin of aged animals *in vivo*. The results showed that continuous nsPEF stimulation for 14 days effectively enhanced the number of mature blood vessels in the skin of both naturally aged (20-month-old SD rats) and metabolically aged (D-galactose-induced C57 mice) animals, showing more than a 2-fold increase as evidenced by α-SMA staining, a marker of mature vasculature (Fig. 5). Notably, nsPEF treatment successfully restored the number of mature blood vessels to levels comparable to those in normal skin tissue. Additionally, we co-stained the MNRC proteins HIF-1α and SIRT1 with the ECs marker CD31 to find whether nsPEF promotes angiogenesis by influencing the expression of MNRC mediators in vascular endothelial cells. The results showed that on day 7 of continuous nsPEF stimulation, nsPEF stimulations increased the expression of MNRC mediators HIF-1α and SIRT1 in the skin blood vessels ECs of both aged animal models (Fig. 6). These *in vivo* findings are consistent with the above-reported *in vitro* cellular experimental results.

4. Discussion

Mitochondrial dysfunction plays a key role in ECs aging, particularly through the disruption of MNRC [30]. HIF-1α and SIRT1 are crucial mediators of this retrograde signaling, regulating the expression of genes involved in processes such as VEGF signaling and cell proliferation, which are vital for angiogenesis [31–34]. As a physical therapeutic approach, nsPEF applications exert two kinds of biological effects on cells, i.e., low-intensity nsPEF treatments can activate the proliferation and differentiation of normal cells [35–38], and higher-intensity nsPEF exposures lead to cell death [39–42]. Current models have confirmed that nsPEF penetrates the cell plasma membrane and affects mitochondrial function [43,44]. Under high-intensity conditions, nsPEFs can trigger mitochondrial apoptosis pathways [40,45,46], a feature that has been widely applied in cancer treatments. However, it is still unclear whether the effects of the promotion of cell proliferation and differentiation by low-intensity nsPEF exposures are based on modulating mitochondrial MNRC. Previously, the effects of low-intensity nsPEF treatments on aging cells had not been documented. Therefore, this study investigated whether nsPEF applications could activate MNRC mediators HIF-1α and SIRT1 to restore ECs proliferation and promote angiogenesis in aged skin.

While the proliferative effects of nsPEFs on suspended cells had been previously reported, only limited research explored its effects on *in vitro* adherent cells and *in vivo* models [35,37,47]. To better mimic the physiological growth conditions of cells *in vivo*, we developed a nsPEF system for both *in vitro* adherent cells and animal models, including optimized treatment parameters and cycles, to explore the mechanisms through which nsPEF promotes cell growth. In this study, we observed that the D-galactose-induced aging phenotype in HUVECs included a significant reduction in the expression of HIF-1α and SIRT1 proteins, thereby disrupting the normal MRNC. Consistent with previous research [35], this disruption was associated with increased oxidative stress and functional impairment, leading to cellular aging [23,27]. Upon applying the nsPEF, a significant increase in mitochondrial membrane potential was detected after 6 h of treatment (Fig. 3), which is known to trigger MNRC [12]. Consistent with this, after 24 h of

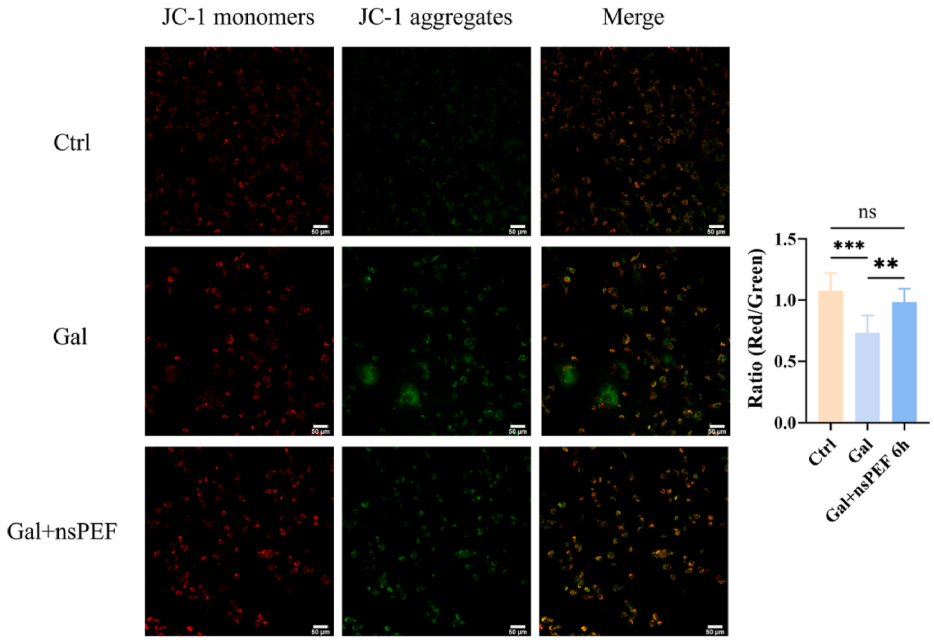

Fig. 3. Effect of nsPEF treatments on mitochondrial membrane potential in D-galactose-induced HUVECs. After nsPEF treatments, cells were further cultured for 6 h before staining. An increase in mitochondrial membrane potential was shown by the formation of JC-1 aggregates, which emitted a red fluorescence. A decrease in mitochondrial membrane potential was revealed by the formation of JC-1 monomers, which emitted a green fluorescence. Ctrl: Normal cultured HUVECs. Gal: Aging HUVECs induced by D-galactose for 48 h, followed by normal culture for 6 h. Gal + nsPEF: Aging HUVECs treated with nsPEF, followed by normal culture for 6 h. Bar length = 50 μm, n = 3 per group. In the statistical chart of the red/green fluorescence intensity ratio of JC-1 staining, $^{**}P < 0.01$, $^{***}P < 0.001$.

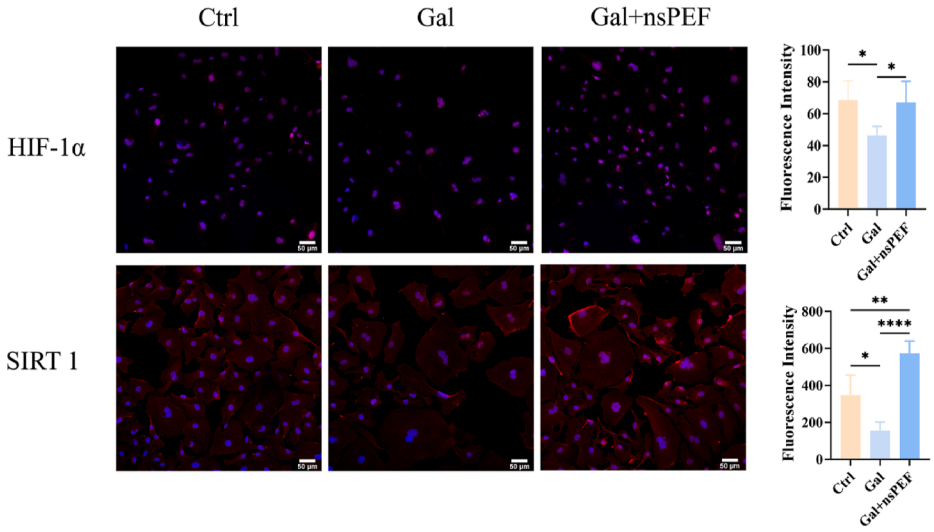

Fig. 4. The enhancing effect of nsPEF treatments on the expression levels of two key MNRC-related proteins in D-Galactose-induced aging HUVECs. Target proteins emit a red fluorescence, while the cell nuclei blue one. Following nsPEF treatments, the cells were cultured for an additional 24 h prior to staining. *Abbreviations*: Ctrl, Normal cultured HUVECs. Gal, Aging HUVECs induced by D-galactose for 48 h, followed by a normal culture for 24 h. Gal + nsPEF, Aging HUVECs treated with nsPEF, followed by a normal culture for 24 h. Scale bar = 50 μm, n = 3 per group, $*P < 0.05$, $***P < 0.001$, $****P < 0.0001$.

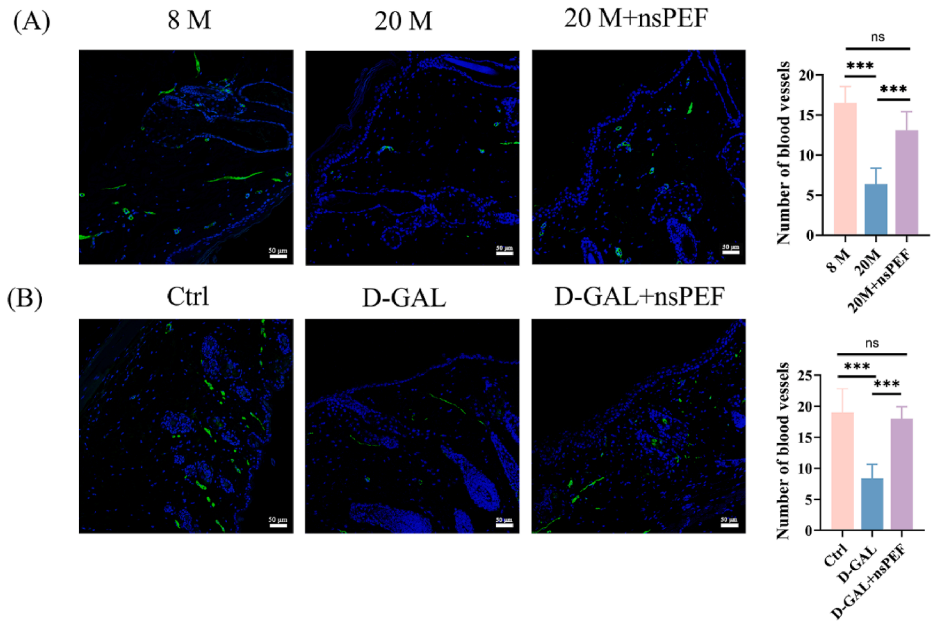

Fig. 5. The nsPEF treatments stimulate skin angiogenesis in different aged rodent models. (A) α-SMA fluorescence staining of skin tissue from 20-month-old (20 M) SD rats following nsPEF stimulations. 8-Month-old (8 M) SD rats were used as the young control group. Scale bar = 50 μm. (B) α-SMA fluorescence staining of skin tissue from D-galactose-induced C57 mice following nsPEF stimulation. Age-matched untreated mice served as the Ctrl group. Scale bar = 50 μm, n = 3 per group, $***P < 0.001$.

treatment, the expression levels of HIF-1α and SIRT1 proteins were significantly elevated (Fig. 4). The observed increases in the expression of these two proteins suggest that nsPEF restored mitochondrial MNRC. These retrograde signals triggered the expression of genes modulating antioxidant stress, cell proliferation, and repair in according to current needs. Thus, after 48 h, nsPEF treatment successfully reversed oxidative stress (Fig. 2C) and mitotic cell cycle arrest (Fig. 2B) in aging HUVECs. These findings suggest that nsPEF treatments may favor neoangiogenesis. Therefore, we confirmed this finding in two rodent models, one of natural aging (20-month-old SD rats) and one of metabolic aging (D-galactose-induced C57 mice). In these aged models, nsPEF stimulations upregulated ECs' expression of HIF-1α and SIRT1 (Fig. 6) and promoted neoangiogenesis in the skin tissue (Fig. 5). The consistency between *in vitro* and *in vivo* findings holds up the therapeutic potential of nsPEF treatments in restoring vascular ECs' function.

Rejuvenation refers to giving aged cells or organisms more youthful characteristics through various techniques [48]. Specifically, rejuvenation is the reversal of aging and thus requires a different strategy, namely repair of the damage that is associated with aging or replacement of damaged tissue with new tissue [49]. According to the updated conceptual framework of aging, fourteen recognized hallmarks have been identified, including cellular

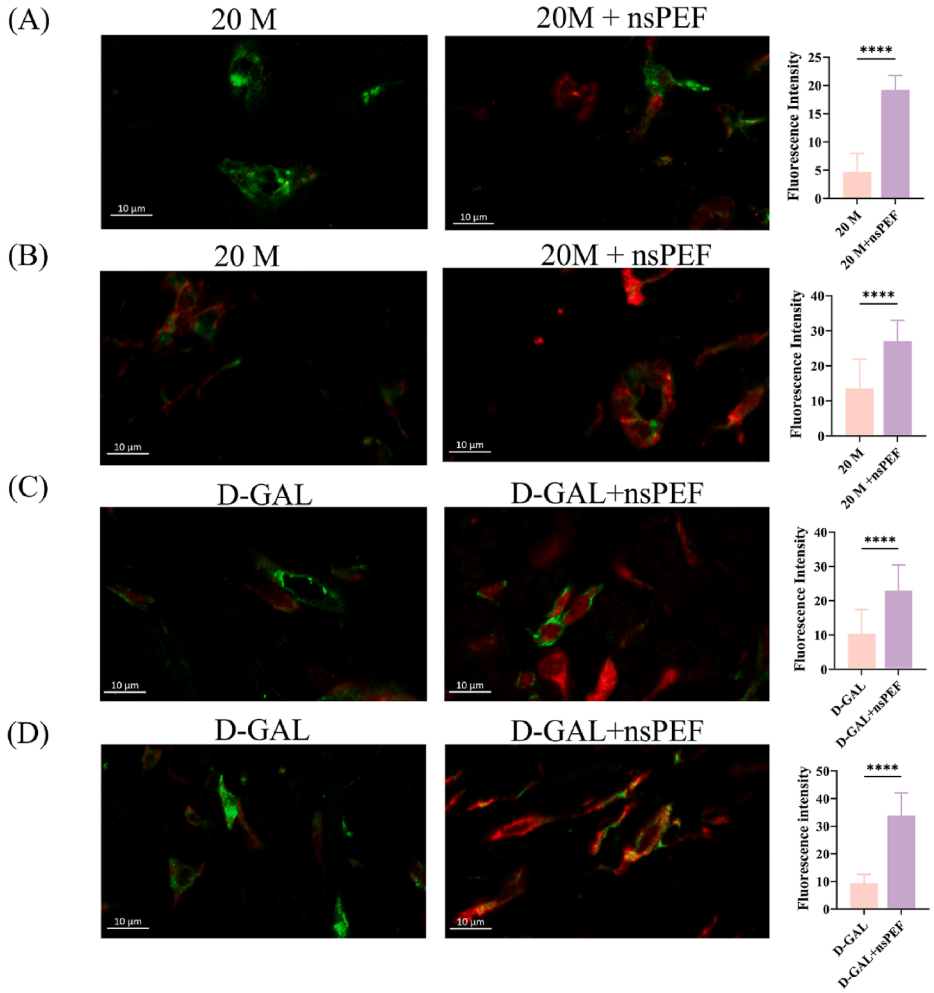

Fig. 6. The nsPEF treatments stimulate the expression of MNRC mediator proteins HIF-1α and SIRT1 in skin ECs from different aged rodent models. (A) CD31 (green) and HIF-1α (red) fluorescence staining of skin tissue from 20-month-old SD rats following nsPEF stimulations. Scale bar = 10 μm. (B) CD31 (green) and SIRT1 (red) fluorescence staining of skin tissue from 20-month-old SD rats following nsPEF stimulations. Scale bar = 10 μm. (C) CD31 (green) and HIF-1α (red) fluorescence staining of skin tissue from D-galactose-induced C57 mice following nsPEF stimulations. Scale bar = 10 μm. (D) CD31 (green) and SIRT1 (red) fluorescence staining of skin tissue from D-galactose-induced C57 mice following nsPEF stimulations. The region of interest (ROI) was defined manually based on the area showing green fluorescence. The fluorescence intensity within each ROI was measured using ImageJ. Scale bar = 10 μm, n = 3 per group, ***$P < 0.001$.

senescence, mitochondrial dysfunction, genomic instability, telomere attrition, epigenetic alterations, loss of proteostasis, deregulated nutrient sensing, stem cell exhaustion, altered intercellular communication, impaired autophagy, chronic inflammation, microbiome dysbiosis, extracellular matrix remodeling, and social isolation [50]. The molecular pathways underlying these hallmarks are intricately interconnected, such that interventions targeting a single hallmark often exert beneficial effects on others, thereby collectively delaying the progression of aging-related phenotypes [7]. In the present study, our results demonstrated that nsPEF exert anti-endothelial aging effects primarily by ameliorating mitochondrial dysfunction (an increase in mitochondrial membrane potential, along with a concomitant reduction in ROS levels), which in turn may attenuate other aging-associated hallmarks, such as cellular senescence (a significant reduction in SA-β-Gal activity). Moreover, through this mechanism, nsPEF promoted angiogenesis in aged skin tissues. Based on the aforementioned definition of rejuvenation as the reversal of aging-related damage and the restoration of youthful function, these findings suggest that nsPEF represents a promising strategy for promoting the rejuvenation of vascular endothelial cells.

Interestingly, our study revealed that the nsPEF parameters capable of rejuvenating aging ECs had no significant effect on normal (untreated) cells. It contrasts with previous studies, which reported that low-intensity nsPEF promotes proliferation and differentiation in normal cells. However, these discrepant findings may be due to the different nsPEF parameters respectively used: this study applied 3 kV/cm, while earlier studies used 5 kV/cm [27]. The biological effects induced by nsPEF treatments can vary significantly according to the electric field parameters, as well as the specific characteristics of the target cells or tissues [51]. Additionally, the electrophysiological properties, such as cell morphology, membrane capacitance, and membrane resistance, of aging cells differ from those proper of young/adult normal cells. These differences make aging cells more sensitive to the lower nsPEF intensities used in this study, enabling the restoration of their function while not affecting normal cells. This underscores the importance of carefully selecting the nsPEF parameters to optimize the "therapeutic window", which ensures the effective treatment of the target cells or tissues while minimizing the risk of damaging healthy cells. This consideration is crucial for the safe and effective application of nsPEF in biomedical treatments.

Future studies should focus on elucidating the specific mechanisms by which nsPEF applications modulate mitochondrial membrane potential and activate MNRC. This may involve investigating direct alterations to the mitochondrial membrane proteome or function, changes in mitochondrial membrane potential difference, and shifts in the distribution of calcium ions. These investigations will offer important insights into the biological effects of nsPEF and help develop more refined therapeutic strategies for age-related diseases.

5. Conclusion

The current study proved that nsPEF rescues aging ECs by restoring MNRC in both *in vitro* and *in vivo* models. Our work shows that nsPEF under certain doses could serve as the mitochondrial function "activator," which might be promising in the treatment of age-related diseases.

Ethical approval

All animal experiments in this study were approved by the Animal Welfare and Ethics Committee of China Resources Group Co. Ltd. (Shenzhen) (Approval No. 202300122).

Consent for publication

The authors participated in this study were all consented for the publication.

Data availability statement

The data that support the findings of this study are available from the corresponding author upon reasonable request.

Declaration of competing interest

The authors declare that they have no known competing financial interests or personal relationships that could have appeared to influence the work reported in this paper.

Acknowledgments

This study has received funding by Shenzhen High-level Hospital Construction Fund (Grant No.4004006), Sanming project of Medicine in Shenzhen (Grant No. SZSM202111020), National Natural Science Foundation of China (Grant No.82172214) and National Key Research and Development Program (Grant No.2022YFC2403101).

References

[1] Chen J, Sivan U, Tan SL, Lippo L, De Angelis J, Labella R, et al. High-resolution 3D imaging uncovers organ-specific vascular control of tissue aging. Sci Adv 2021;7:eabd7819.
[2] Augustin HG, Koh GY. A systems view of the vascular endothelium in health and disease. Cell 2024;187:4833–58.
[3] Chung JH, Eun HC. Angiogenesis in skin aging and photoaging. J Dermatol 2007;34:593–600.
[4] Szpalski C, Butala P, Vandegrift MT, Knobel D, Allen RJJ, Saadeh PB, et al. Improving senescent wound healing with local and systemic therapies. Ann Plast Surg 2018;81:96–105.
[5] Faconti L, Bruno RM, Ghiadoni L, Taddei S, Virdis A. Ventricular and vascular stiffening in aging and hypertension. Curr Hypertens Rev 2015;11:100–9.
[6] Ge Y. Vascular contributions to healthy aging and dementia. Aging Dis 2024;15:1432–7.
[7] López-Otín C, Blasco MA, Partridge L, Serrano M, Kroemer G. Hallmarks of aging: an expanding universe. Cell 2023;186:243–78.
[8] Zhu D, Li X, Tian Y. Mitochondrial-to-nuclear communication in aging: an epigenetic perspective. Trends Biochem Sci 2022;47:645–59.
[9] De Stefani D, Rizzuto R, Pozzan T. Enjoy the trip: calcium in mitochondria back and forth. Annu Rev Biochem 2016;85:161–92.
[10] Liu Z, Butow RA. Mitochondrial retrograde signaling. Annu Rev Genet 2006;40:159–85.
[11] Vizioli MG, Liu T, Miller KN, Robertson NA, Gilroy K, Lagnado AB, et al. Mitochondria-to-nucleus retrograde signaling drives formation of cytoplasmic chromatin and inflammation in senescence. Genes Dev 2020;34:428–45.
[12] Sakamuru S, Zhao J, Attene-Ramos MS, Xia M. Mitochondrial membrane potential assay. Methods Mol Biol 2022;2474:11–9.
[13] Hill S, Van Remmen H. Mitochondrial stress signaling in longevity: a new role for mitochondrial function in aging. Redox Biol 2014;2:936–44.
[14] Walker BR, Moraes CT. Nuclear-mitochondrial interactions. Biomolecules 2022;12.
[15] Chang H, Ou Yang R, Su J, Nguyen TMH, Sung J, Tang M, et al. YAP nuclear translocation induced by HIF-1α prevents DNA damage under hypoxic conditions. Cell Death Discov 2023;9:385.
[16] Depping R, Steinhoff A, Schindler SG, Friedrich B, Fagerlund R, Metzen E, et al. Nuclear translocation of hypoxia-inducible factors (HIFs): involvement of the classical importin alpha/beta pathway. Biochim Biophys Acta 2008;1783:394–404.
[17] Alique M, Sánchez-López E, Bodega G, Giannarelli C, Carracedo J, Ramírez R. Hypoxia-inducible factor-1α: the master regulator of endothelial cell senescence in vascular aging. Cells 2020;9.
[18] Alique M, Bodega G, Giannarelli C, Carracedo J, Ramírez R. MicroRNA-126 regulates Hypoxia-inducible factor-1α which inhibited migration, proliferation, and angiogenesis in replicative endothelial senescence. Sci Rep 2019;9:7381.
[19] Yang Y, Liu Y, Wang Y, Chao Y, Zhang J, Jia Y, et al. Regulation of SIRT1 and its roles in inflammation. Front Immunol 2022;13:831168.
[20] Chen C, Zhou M, Ge Y, Wang X. SIRT1 and aging related signaling pathways. Mech Ageing Dev 2020;187:111215.
[21] Wang L, Xu C, Johansen T, Berger SL, Dou Z. SIRT1 - a new mammalian substrate of nuclear autophagy. Autophagy 2021;17:593–5.
[22] Zu Y, Liu L, Lee MYK, Xu C, Liang Y, Man RY, et al. SIRT1 promotes proliferation and prevents senescence through targeting LKB1 in primary porcine aortic endothelial cells. Circ Res 2010;106:1384–93.
[23] Campagna R, Mazzanti L, Pompei V, Alia S, Vignini A, Emanuelli M. The multifaceted role of endothelial sirt1 in vascular aging: an Update. Cells 2024;13.
[24] Ruiz-Fernández AR, Campos L, Gutierrez-Maldonado SE, Núñez G, Villanelo F, Perez-Acle T. Nanosecond pulsed electric field (nsPEF): opening the biotechnological pandora's box. Int J Mol Sci 2022;23.
[25] Chen N, Garner AL, Chen G, Jing Y, Deng Y, Swanson RJ, et al. Nanosecond electric pulses penetrate the nucleus and enhance speckle formation. Biochem Biophys Res Commun 2007;364:220–5.
[26] Rems L, Ušaj M, Kandušer M, Reberšek M, Miklavčič D, Pucihar G. Cell electrofusion using nanosecond electric pulses. Sci Rep 2013;3:3382.
[27] Zhang Y, Dong F, Liu Z, Guo J, Zhang J, Fang J. Nanosecond pulsed electric fields promoting the proliferation of porcine iliac endothelial cells: an in vitro study. PLoS One 2018;13:e196688.
[28] Lee G, Hoang T, Jung E, Jung S, Han S, Chung M, et al. Anthocyanins attenuate endothelial dysfunction through regulation of uncoupling of nitric oxide synthase in aged rats. Aging Cell 2020;19:e13279.
[29] Radwan B, Rocchetti S, Matuszyk E, Sternak M, Stodulski M, Pawlowski R, et al. EdU sensing: the Raman way of following endothelial cell proliferation in vitro and ex vivo. Biosens Bioelectron 2022;216:114624.
[30] Martini H, Passos JF. Cellular senescence: all roads lead to mitochondria. FEBS J 2023;290:1186–202.
[31] Tang N, Wang L, Esko J, Giordano FJ, Huang Y, Gerber H, et al. Loss of HIF-1alpha in endothelial cells disrupts a hypoxia-driven VEGF autocrine loop necessary for tumorigenesis. Cancer Cell 2004;6:485–95.
[32] Karshovska E, Zernecke A, Sevilmis G, Millet A, Hristov M, Cohen CD, et al. Expression of HIF-1alpha in injured arteries controls SDF-1alpha mediated neointima formation in apolipoprotein E deficient mice. Arterioscler Thromb Vasc Biol 2007;27:2540–7.
[33] Mengozzi A, Costantino S, Paneni F, Duranti E, Nannipieri M, Mancini R, et al. Targeting SIRT1 rescues age- and obesity-induced microvascular dysfunction in ex vivo human vessels. Circ Res 2022;131:476–91.
[34] Guarani V, Potente M. SIRT1 - a metabolic sensor that controls blood vessel growth. Curr Opin Pharmacol 2010;10:139–45.
[35] Ning T, Guo J, Zhang K, Li K, Zhang J, Yang Z, et al. Nanosecond pulsed electric fields enhanced chondrogenic potential of mesenchymal stem cells via JNK/CREB-STAT3 signaling pathway. Stem Cell Res Ther 2019;10:45.
[36] Han J, Wang Z, Dong Y, Zou X, Wang H, Chen Y, et al. Regulating schwann cell growth by nanosecond pulsed electric field for peripheral nerve regeneration in vitro. J Vis Exp 2024 May 3;207. https://doi.org/10.3791/66097.
[37] Vadlamani RA, Nie Y, Detwiler DA, Dhanabal A, Kraft AM, Kuang S, et al. Nanosecond pulsed electric field induced proliferation and differentiation of osteoblasts and myoblasts. J R Soc Interface 2019;16:20190079.
[38] Zhang K, Guo J, Ge Z, Zhang J. Nanosecond pulsed electric fields (nsPEFs) regulate phenotypes of chondrocytes through Wnt/β-catenin signaling pathway. Sci Rep 2014;4:5836.
[39] Guo J, Wang Y, Wang J, Zhang J, Fang J. Radiosensitization of oral tongue squamous cell carcinoma by nanosecond pulsed electric fields (nsPEFs). Bioelectrochemistry 2017;113:35–41.

[40] Asadipour K, Hani MB, Potter L, Ruedlinger BL, Lai N, Beebe SJ. Nanosecond pulsed electric fields (nsPEFs) modulate electron transport in the plasma membrane and the mitochondria. Bioelectrochemistry 2024;155:108568.
[41] Beebe SJ, Chen Y, Sain NM, Schoenbach KH, Xiao S. Transient features in nanosecond pulsed electric fields differentially modulate mitochondria and viability. PLoS One 2012;7:e51349.
[42] Batista Napotnik T, Wu Y, Gundersen MA, Miklavčič D, Vernier PT. Nanosecond electric pulses cause mitochondrial membrane permeabilization in Jurkat cells. Bioelectromagnetics 2012;33:257–64.
[43] Kotnik T, Miklavcic D. Theoretical evaluation of voltage inducement on internal membranes of biological cells exposed to electric fields. Biophys J 2006;90:480–91.
[44] Guo F, Zhang L, Liu X. Nonlinear dispersive cell model for microdosimetry of nanosecond pulsed electric fields. Sci Rep 2020;10:19456.
[45] Fan A, Liu G, Wu X. Nanosecond pulse electric field treatment initiates mitochondrial apoptosis pathway by inducing mitochondrial morphological changes in myocardial cells. J Intervent Card Electrophysiol 2024 Aug 2. https://doi.org/10.1007/s10840-024-01828-5.
[46] Ford WE. Nanosecond pulsed electric fields induce a mitochondria-independent apoptosis in B16F10 Melanoma Cells in Vitro. 2008.
[47] Li K, Ning T, Wang H, Jiang Y, Zhang J, Ge Z. Nanosecond pulsed electric fields enhance mesenchymal stem cells differentiation via DNMT1-regulated OCT4/NANOG gene expression. Stem Cell Res Ther 2020;11:308.
[48] Ji S, Xiong M, Chen H, Liu Y, Zhou L, Hong Y, et al. Cellular rejuvenation: molecular mechanisms and potential therapeutic interventions for diseases. Signal Transduct Targeted Ther 2023;8:116.
[49] Hass R. Rejuvenation in distinct cell populations - what does it mean? Exp Gerontol 2009;44:634–8.
[50] Kroemer G, Maier AB, Cuervo AM, Gladyshev VN, Ferrucci L, Gorbunova V, et al. From geroscience to precision geromedicine: understanding and managing aging. Cell 2025;188:2043–62.
[51] Ning T, Zhang K, Heng BC, Ge Z. Diverse effects of pulsed electrical stimulation on cells - with a focus on chondrocytes and cartilage regeneration. Eur Cell Mater 2019;38:79–93.